Do biotransformation data from laboratory experiments reflect micropollutant degradation in a large river basin?

Seller, Carolin ; Varga, Laura ; Börgardts, Elizabeth ; Vogler, Bernadette ; Janssen, Elisabeth ; Singer, Heinz ; Fenner, Kathrin ; Honti, Mark

DOI: https://doi.org/10.1016/j.watres.2023.119908

Water Research 235 (2023) 119908

Contents lists available at ScienceDirect

Water Research

journal homepage: www.elsevier.com/locate/watres

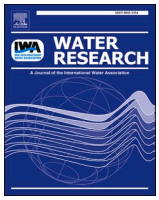

Do biotransformation data from laboratory experiments reflect micropollutant degradation in a large river basin?

Carolin Seller [a,b], Laura Varga [c], Elizabeth Börgardts [a], Bernadette Vogler [a], Elisabeth Janssen [a], Heinz Singer [a], Kathrin Fenner [a,b,*], Mark Honti [d,**]

[a] Eawag, Swiss Federal Institute of Aquatic Science and Technology, 8600 Dübendorf, Switzerland
[b] Department of Chemistry, University of Zürich, 8057 Zürich, Switzerland
[c] Department of Sanitary and Environmental Engineering, Budapest University of Technology and Economics, 1111 Budapest, Hungary
[d] ELKH-BME Water Research Group, 1111 Budapest, Hungary

ARTICLE INFO

Keywords:
Biotransformation kinetics
Laboratory-field comparison
Micropollutants
Bayesian model frameworks

ABSTRACT

Identifying a chemical's potential for biotransformation in the aquatic environment is crucial to predict its fate and manage its potential hazards. Due to the complexity of natural water bodies, especially river networks, biotransformation is often studied in laboratory experiments, assuming that study outcomes can be extrapolated to compound behavior in the field. Here, we investigated to what extent outcomes of laboratory simulation studies indeed reflect biotransformation kinetics observed in riverine systems. To determine in-field biotransformation, we measured loads of 27 wastewater treatment plant effluent-borne compounds along the Rhine and its major tributaries during two seasons. Up to 21 compounds were detected at each sampling location. Measured compound loads were used in an inverse model framework of the Rhine river basin to derive $k'_{bio,field}$ values – a compound-specific parameter describing the compounds' average biotransformation potential during the field studies. To support model calibration, we performed phototransformation and sorption experiments with all the study compounds, identifying 5 compounds that are susceptible towards direct phototransformation and determining K_{oc} values covering four orders of magnitude. On the laboratory side, we used a similar inverse model framework to derive $k'_{bio,lab}$ values from water-sediment experiments run according to a modified OECD 308-type protocol. The comparison of $k'_{bio,lab}$ and $k'_{bio,field}$ revealed that their absolute values differed, pointing towards faster transformation in the Rhine river basin. Yet, we could demonstrate that relative rankings of biotransformation potential and groups of compounds with low, moderate and high persistence agree reasonably well between laboratory and field outcomes. Overall, our results provide evidence that laboratory-based biotransformation studies using the modified OECD 308 protocol and k'_{bio} values derived thereof bear considerable potential to reflect biotransformation of micropollutants in one of the largest European river basins.

1. Introduction

Wastewater treatment plants (WWTPs) often discharge their effluents into rivers and streams, resulting in exposure of riverine ecosystems to chemicals (Hamdhani et al., 2020). Actual exposure levels and the individual chemical's potential to cause damage to these ecosystems depends on their mass load in the WWTP effluents and the extent to which they can be removed from the aquatic environment via biotic and abiotic transformation (Berkner and Thierbach 2014; Fenner et al., 2013; Schwarzenbach et al., 2006). Therefore, a chemical's persistence, i.e., recalcitrance towards transformation in aquatic environments, is considered a key hazard property in chemical regulations worldwide (Cousins et al., 2019).

Yet, directly quantifying transformation of chemicals in rivers is challenging for several reasons. First, especially in industrialized and densely populated regions, distances and hence hydraulic residence times between WWTPs along rivers are typically short. Unless a compound is transformed at a very high rate and its transformation can therefore be observed along the short distance between two WWTPs, new emissions from WWTPs will overlay upstream compound loads and

* Corresponding author at: Eawag, Swiss Federal Institute of Aquatic Science and Technology, Dübendorf 8600, Switzerland.
** Corresponding author.
E-mail addresses: kathrin.fenner@eawag.ch (K. Fenner), mark.honti@gmail.com (M. Honti).

https://doi.org/10.1016/j.watres.2023.119908
Received 31 August 2022; Received in revised form 20 February 2023; Accepted 22 March 2023
Available online 22 March 2023

mask the transformation signal. Second, chemical concentrations are modulated by dilution in river networks, which needs to be explicitly accounted for to quantify compound loads and hence removal. Lastly, while a chemical's structure determines to some extent its potential to be transformed, the actual extent of transformation in a riverine environment is additionally influenced by the chemical's bioavailability, the environmental conditions such as pH and temperature, and, in the case of biotransformation, the abundance of enzymes and/or competent microbial degraders that can transform a given chemical structure. Both, environmental conditions as well as microbial community composition and activity, are known to vary spatially and temporally (Chalifour et al., 2021; Fenner et al., 2013; Gao et al., 2019; Helbling et al., 2012; Winter et al., 2007). Indeed, previous field studies showed large variabilities in compound attenuation from different sections of various European rivers, rendering it almost impossible to derive conclusive evidence regarding a chemical's environmental persistence from the observation of riverine concentrations alone (Jaeger et al., 2019; Li et al., 2016).

For all of these reasons, persistence of chemicals is most often studied in laboratory experiments under controlled conditions. Since aerobic biotransformation is considered the dominant removal pathway for most commonly detected chemical pollutants, it is common practice to use laboratory biotransformation studies following internationally accepted OECD guidelines to assess aquatic persistence. This practice is based on the assumption that laboratory observations are representative of compound behavior in the field. Yet, the robustness of this assumption has barely been addressed in previous research (Adriaanse et al., 1997; Montforts 2006). In fact, the few attempts to relate outcomes of, e.g., OECD 308 water-sediment studies to compound behavior in riverine environments remained inconclusive (Honti et al., 2018a; Radke and Maier 2014b; Southwell et al., 2020).

Recently, Shrestha et al. (2016, 2021) introduced, broadly tested, and characterized a novel laboratory system in which a thin predominantly aerobic sediment layer is covered by an aerated water column favoring aerobic biotransformation as dominant compound removal pathway (referred to as modified OECD 308-type study in Seller et al. (2021)). It has been argued that such a laboratory system may be well suited to elucidate a chemical's potential for biotransformation in riverine environments, i.e., in fully mixed water bodies with the first few centimeters of sediment being aerobic (Seller et al., 2021) – however, this hypothesis has not yet been tested and warrants further exploration. Therefore, the primary aim of this study was to investigate to what extent outcomes of modified OECD 308-type studies can be compared to biotransformation kinetics of chemicals observed in riverine systems across a large number of relevant aquatic pollutants.

To fulfill this aim, a sound basis for comparison of laboratory and field biotransformation had to be sought. Transformation half-lives (DT_{50}), while being essential pieces of information in a regulatory context, typically lump together transformation and phase transfer processes, particularly in water-sediment systems, and are system-specific in many aspects (i.e., dependent on, e.g., water-sediment ratios, suspended solids concentration, or sediment total organic carbon (TOC)), making them unfit for comparison of biotransformation between laboratory test systems and river environments (Honti et al., 2016). To eliminate some of the most influential system-specific differences affecting aquatic biotransformation, Honti et al. (2016, 2018a) introduced k'_{bio}, a biomass-corrected second-order rate constant. k'_{bio} is estimated from measured chemical concentration patterns and information on the physicochemical properties of, and biomass in, the studied system through inverse modeling. It hinges on the assumption that total biomass – or, in case such information is missing, TOC – can serve as proxies for the abundance of degrading enzymes and/or competent microbial degraders. Since k'_{bio} is also corrected for differences in the chemical's bioavailability in water-sediment systems exhibiting different sediment-to-water ratios, it should, in principle, allow comparing a chemical's biotransformation potential across laboratory and field systems. Yet, previous attempts to derive k'_{bio} from field observations in the Rhine river catchment were subject to large uncertainties mostly due to a substantial lack of accurately known compound emissions into the Rhine but also due to a lack of precise knowledge on other relevant fate properties that are required for the inverse estimation of k'_{bio}. Those include the compounds' susceptibility towards abiotic transformation (i.e., hydrolysis and photo-transformation) and their organic carbon-water partition coefficient (K_{oc}) influencing the compounds' (estimated) bioavailability (Honti et al., 2018a). Therefore, in order to apply the k'_{bio}-concept for comparing chemicals' biotransformation kinetics between laboratory studies and riverine environments, a secondary aim of this work was to improve the estimation of k'_{bio} from monitored river concentration in the catchment of the river Rhine, one of the largest and most important catchments of Europe.

To this end, we (i) conducted sorption and phototransformation laboratory experiments to provide sufficiently accurate data describing the compounds' abiotic fate properties, (ii) determined weekly compound loads in the main channel of the Rhine and its major tributaries in Switzerland, Germany, and the Netherlands during catchment-wide field campaigns in spring and summer 2017, and (iii) estimated compound emission into the Rhine based on an effluent monitoring-based approach presented by Varga et al. (2023). Finally, we inferred k'_{bio} values from the Rhine field study ($k'_{bio,field}$) and from modified OECD 308-type studies ($k'_{bio,lab}$) using inverse model frameworks and systematically compared model outcomes to evaluate to what extent biotransformation data from laboratory experiments reflect micropollutant degradation in a large river basin.

2. Materials and methods

2.1. Test compounds

Based on the compound selection of Seller et al. (2021), $k'_{bio,lab}$ values describing biotransformation in modified OECD 308-type studies were derived for 42 compounds, including 23 pharmaceuticals, 15 pesticides, 3 artificial sweeteners, and 1 industrial chemical. $k'_{bio,field}$ values describing biotransformation in the Rhine river catchment were inferred for a subset of 27 compounds that were expected to be released into the aquatic environment via WWTP effluents, i.e., pharmaceuticals, artificial sweeteners, and industrial chemicals (here referred to as "field compounds"). It has to be noted that the here employed analytical methods did not allow to differentiate between 4- and 5-methylbenzotriazole and, therefore, compound loads measured in the Rhine river catchment are most likely a combination of both (Ruff et al., 2015). A list of all compounds, including name abbreviations, is provided in Table SI1.

2.2. Experimental and field data of test compounds

2.2.1. Compound loads in the Rhine catchment

To determine the field compounds' abundance and transformation behavior within the Rhine river catchment, this study benefited from the activities of the International Commission for the Protection of the Rhine (IKSR) in the frame of the sampling campaign "Sondermessprogramm Chemie" (SMPC) (IKSR 2019). During the SMPC, four water parcels were tracked along the Rhine during each season of 2017. The water parcels were sampled by means of weekly composite samples at eleven locations within the main channel of the Rhine and at six locations along its major tributaries close to their confluence points with the Rhine (Table SI2 and Fig. SI1). We received samples from two of the four SMPC campaigns, i.e., from the P1 campaign with samples taken between March 19th – April 6th, 2017, and from the P3 campaign with samples taken between July 10th–27th, 2017. We measured concentrations of field compounds using an Agilent 6495C Triple Quad Mass Spectrometer coupled to an Agilent HPLC 1290 (binary pump) system (SI1.3).

Compound loads were calculated by multiplying the concentrations measured in the IKSR samples with the discharge measured at each sampling time and location (Table SI10 - Table SI13).

2.2.2. Data from biotransformation simulation studies

Data provided by Seller et al. (2021) describe compound behavior in modified OECD 308-type studies, i.e., in systems in which a sediment layer was covered by an aerated water column to a sediment-water ratio of 1:10 (v/v) (further information provided in SI1.4). Inocula for modified OECD 308-type studies were sampled from two locations, i.e., a WWTP effluent-impacted river and a pristine pond. We used compound concentrations measured during >54 days of biotransformation experiments in both sediment and water phase to derive $k'_{bio,lab}$ values as described in 2.3.2.

2.3. Biotransformation kinetics modelling frameworks

2.3.1. Determination of $k'_{bio,field}$ values

To derive $k'_{bio,field}$ values, we used the catchment-scale water quality model of Honti et al. (2018a) and extended the model framework with abiotic hydrolysis and direct phototransformation as potential removal pathways for dissolved parent compounds (please note that we experimentally studied our field compounds' susceptibility towards indirect phototransformation and, based on the results, decided to neglect indirect phototransformation as a potential compound removal pathway for the selected field compounds from the Rhine river catchment, see 3.1.1). The most important underlying assumptions of the Rhine catchment model are (i) that only dissolved compound mass fractions are available for abiotic and biotic transformation following a first-order decay and (ii) that converting $k'_{bio,field}$ into compound-specific degradation rate constants requires considering degrader biomass. Total organic carbon (TOC) estimates were used as a proxy for degrader biomass as previous studies were able to link organic carbon content of river bed sediments to microbial activity (Fischer et al., 2002). The Rhine catchment model is based on individual river reaches described by the Catchment Characterization Model Europe (CCM2) (De Jager and Vogt, 2007). In each reach, partitioning and transformation at equilibrium are described as functions of the physical properties of the reach and the sorption/ transformation properties of the field compounds. A compound's behavior in the entire catchment of the river Rhine was then simulated by connecting the >18.000 stream reaches following the topology of the stream network. In each reach, the output compound flux was calculated as:

$$F_{out} = F_{in} \exp(-\delta\, \tau_w\, k_w) \quad (1)$$

where F_{in} and F_{out} [kg d^{-1}] are the incoming and outflowing fluxes of the parent compound for a single reach, respectively, and τ_w [d] is the compounds' mean water residence time in a reach. k_w [d^{-1}] is the compound's transformation rate constant in water, considering rate constants describing abiotic hydrolysis ($k_{hydro,TS}$) and phototransformation ($k'_{photo,TS}$), together with biotransformation ($k'_{bio,field}$) in the total system (TS) (SI1.7). δ [-] is a modification factor derived from the physical properties of the respective reach and the sorption behavior of the compound:

$$\delta = 1 + \frac{\frac{S}{SSC\ z_w}}{\frac{z_a}{K_{oc}\ f_{oc,sed}\ S} + 1} \quad (2)$$

where K_{oc} [L kg^{-1}] is the organic carbon-water partitioning coefficient, $f_{oc,sed}$ [-] the organic carbon content of the sediment (i.e., assumed to be 1%) Honti et al., 2018a), SSC [kg m^{-3}] the suspended sediment concentration, z_a and z_w [m] are the depth of the active sediment layer and the water column, respectively, and S [kg m^{-2}] is the settled sediment stock in the active layer. Further details on the derivation of model Eqs. (1) and ((2) are provided by Honti et al. (2018a) and are summarized in SI1.7. The new model components, i.e., $k_{hydro,TS}$ and $k_{photo,TS}$, were derived as:

$$k_{hydro,TS} = k_{hydro}\ (f_{aq,w}\ (1 - p_s) + f_{aq,s}\ p_s) \quad (3)$$

$$k_{photo,TS} = k_{photo}\ f_{aq,w} \exp\left(-k_{ext}\ \frac{z_w}{2}\right) \quad (4)$$

where $k_{hydro,TS}$ [d^{-1}] is the total system hydrolysis rate, k_{hydro} [d^{-1}] is the hydrolysis rate of the dissolved fraction, $f_{aq,w} = 1/(1+K_d\ SSC)$ and $f_{aq,s} = 1/(1+S\ K_d/z_a)$ are the dissolved fractions in the river's water column and pore water of the sediment, $p_s = S/(z_w/K_d + SSC\ z_w + S)$ is the fraction of the compound being in the sediment. k_{photo} [d^{-1}] is the phototransformation rate constant of the dissolved fraction at the water surface (i.e., at the top 1 cm), $k_{ext} = (0.22+0.000011\ SSC)$ [m^{-1}] is the estimated diffuse light attenuation coefficient in water (Batuik et al., 2000; Brown 1984; Hass and Davisson 1977; Kromkamp and Peene 2005).

The mean physical properties for each reach in the Rhine river catchment were estimated based on drainage area and channel slope provided by the CCM2 Database. Mean SSCs were derived from estimated channel geometry, flow velocity, and sediment grain size distribution. In reality, SSC is governed by discharge, season, the state of the upstream catchment, and the stage of flood pulses, which together make it highly dynamic. Here, we had to neglect those variabilities as we had no information to model dynamic SSC in the entire stream network.

The model was fitted to field compound loads measured along the Rhine during the two SMPC campaigns P1 and P3, resulting in $k'_{bio,field,P1}$ and $k'_{bio,field,P3}$ values, respectively. Model calibration took place in a Bayesian framework. Parameter priors for calibration of K_{oc} and transformation rate constants were set to capture experimentally determined values as described thereinafter (see 2.4). Parameter posteriors were sampled by Markov Chain Monte Carlo (MCMC) sampling based on the classical Metropolis algorithm, two parallel chains were launched with 4000 steps each, out of which the first 3000 served for burn-in.

2.3.2. Determination of $k'_{bio,lab}$ values

We adapted the model framework of Honti and Fenner (2015) to describe transformation and sorption processes in modified OECD 308-type studies, i.e., a two-compartment system (Seller et al., 2021). We defined the settled sediment layer including pore water as the first compartment, and the supernatant water column, which we assumed to not contain any suspended sediment, as the second compartment. Test compounds were assumed to be either in dissolved phase in the water compartment (i.e., neglecting association with dissolved organic carbon), or in sorbed or dissolved state in the sediment compartment. The model is structurally compatible with the Rhine catchment model as we apply the same underlying assumptions, i.e., that only dissolved compound mass fractions are available for abiotic and biotic transformation following a first-order decay and that $k'_{bio,lab}$ requires normalization to degrader biomass. In line with procedures to derive $k'_{bio,field}$ values, we use TOC measured in the sediment and water compartment of the experimental vessels as a proxy for degrader biomass. However, as the k'_{bio}-concept thrives from an accurate description of degrader biomass, we furthermore explored the possibility to use bacterial cell densities measured during modified OECD 308-type studies (Seller et al., 2021) as proxy for degrader biomass to derive a second set of $k'_{bio,lab}$ values. Generally, we assume that the fraction of active degraders relative to total bacterial biomass is the same in both laboratory inocula. Dispersion and diffusion processes connecting sediment and water compartments were described following Fick's law. Sorption equilibrium in the sediment was assumed to be reached instantaneously and the sediment compartment itself was treated as a fully mixed reactor, i.e., transformation processes were assumed to take place synchronously and at the same rate throughout the entire shallow sediment layer. Following those model assumptions, compound dissipation over time from the water and sediment compartment, respectively, can be described as:

$$\frac{dP_w}{dt} = -\left(k_{hydro} + k'_{bio,lab}\, DB_w\right) P_w - D_p \frac{\frac{P_w}{z_w} - \frac{P_{w,sed}}{z_{sed}}}{\frac{z_{sed}}{2}} \quad (5)$$

$$\frac{dP_{sed}}{dt} = -\left(k_{hydro} + k'_{bio,lab}\, DB_{sed}\right) \frac{1}{1 + K_{oc}\, f_{oc,sed}\, \frac{\rho_b}{\theta}} P_{sed} + D_p \frac{\frac{P_w}{z_w} - \frac{P_{w,sed}}{z_{sed}}}{\frac{z_{sed}}{2}} \quad (6)$$

with P_w and P_{sed} [ng L^{-1}] as parent compound concentration in the water and sediment compartment, respectively, and $P_{w,sed}$ [ng L^{-1}] as parent compound concentration in pore water. The dissolved fraction of parent compound in the sediment compartment is calculated considering the compounds' K_{oc} values [L kg^{-1}], the sediment's organic carbon fraction ($f_{oc,sed}$), sediment bulk density (ρ_b) [kg L^{-1}], and sediment porosity (Θ). Rate constants k_{hydro} [d^{-1}] and $k'_{bio,lab}$ [L (g OC $d)^{-1}$] or [mL (10^9 cells $d)^{-1}$] describe abiotic and biotic transformation, respectively. DB_w and DB_{sed} were proxys for degrader biomass in water and sediment, respectively, i.e., TOC content [g OC L^{-1}] or bacterial cell densities [10^9 cells mL^{-1}], respectively. Parameters z_w and z_{sed} [cm] describe the height of the water and sediment compartment, respectively. D_p [cm^2 d^{-1}] is a diffusion/dispersion coefficient. Contrary to the Rhine catchment model, phototransformation was neglected as potential compound removal pathway, as modified OECD 308-type studies were conducted in the dark.

The model was fitted to concentration-time series obtained from modified OECD 308-type systems with river and pond inocula (Seller et al., 2021). We used a Bayesian parameter estimation framework to calibrate the model for individual river and pond studies separately (i.e., deriving $k'_{bio,lab,r}$ and $k'_{bio,lab,p}$, respectively), and jointly across both studies (i.e., deriving $k'_{bio,lab,joint}$). The joint fit was performed to verify whether the model can fit experimental data from two biotransformation simulation studies with one set of substance-specific parameters, i.e., $k'_{bio,lab,joint}$, k_{hydro}, and K_{oc}. Parameter priors for calibration were set to capture experimentally determined values as described thereinafter (see 2.4). Posterior parameter distributions were sampled by MCMC sampling with 25′000 iterations from which the first 10′000 were dedicated to burn-in.

2.4. Prior parameter estimates for model calibration

Using Bayesian inference for model calibration allows to incorporate prior knowledge on parameter distributions into the calibration process. To calibrate the k'_{bio}-model frameworks, several parameters used to describe transformation kinetics of compounds in modified OECD 308-type studies (i.e., Eqs. (5) and (6)) or in the Rhine river catchment (i.e., Eq. (1)) are assumed to be compound-specific and, hence, less dependent on the system considered. Besides k'_{bio}, those compound-specific parameters are k_{hydro}, k_{photo} and K_{oc} (see 2.4.1 and 2.4.2 for derivation of k_{photo} and K_{oc} prior distributions, respectively). Another set of prior estimates describe parameters specific to the considered system, e.g., SSC, TOC, or sediment porosity (Honti et al., 2018b). To estimate compound emission into the Rhine, we used quarterly compound consumption data available for Switzerland and Germany and a dimensionless "escape factor" (k_{esc}) describing the proportion of marketed compound reaching the Rhine stream network (Table SI7) (Varga et al., 2023). A compilation of all prior estimates is provided in SI2.

2.4.1. Phototransformation experiments and prior estimation of k_{photo}

Calibration of the Rhine catchment model requires a prior estimate for k_{photo}. Therefore, we conducted phototransformation experiments with the goal to semi-quantitatively assess whether direct or indirect phototransformation may be relevant pathways for removal of selected field compounds from the Rhine river catchment. Phototransformation kinetics were determined (i) in buffered nanopure water (5 mM phosphate buffer, pH= 8), (ii) in buffered nanopure water amended with pony lake fulvic acid (PLFA) to a dissolved organic carbon (DOC) concentration of 10 mg L^{-1} to assess the field compounds' potential for indirect phototransformation at elevated DOC loads, and (iii) in river and pond water previously used for modified OECD 308-type studies sterilized by filtration through glass fiber filters with a pore size of 0.2 μm (i.e., DOC concentrations of 2.2 and 1.2 mg L^{-1}, respectively). Field compounds were spiked into different test waters in mixture to individual concentrations of 1 μg L^{-1}. 40 μM furfuryl alcohol (FFA) were added to determine the concentration of the reactive oxygen species $^1O_2$. To monitor light flux during the experiments, a para-nitroanisole/ pyridine (PNA/Pyr) actinometer was used with initial PNA and Pyr concentrations of 10 μM and 0.5 mM, respectively (Laszakovits et al., 2017). Phototransformation experiments were carried out in quartz tubes (25 mL, inner diameter 1.5 cm), which were positioned in a water bath (25 °C) at an 30° angle 40 cm below the light source of a solar simulator (Heraeus model Suntest CPS+) equipped with a xenon arc lamp. Subsamples of 500 μL were taken from each quartz tube before irradiation, and at five time points within 4 h of experiment. Subsamples were spiked with a mixture of internal standards (ISTDs) to a concentration of 500 ng L^{-1} prior to analysis. Dark control samples were used to account for hydrolysis or other non-photochemical losses of the test compounds. Dark controls were kept in 2 mL amber glass vials covered with aluminum foil, and were immersed in the water bath shielded from the light source to be otherwise exposed to the same experimental conditions as the irradiated samples.

During our phototransformation experiments, the light emitted by the solar simulator was approximately half of the strength of peak summer sunlight in central Europe (i.e., Zürich, Switzerland, 408 m above sea level). Further, the solar simulator suitably mimicked the spectral output of natural sunlight as indicated by the good overlap of the irradiance spectra of the solar simulator and natural sunlight spectra from Europe (Fig. SI3).

To derive prior estimates for k_{photo} in the Rhine river catchment, we followed methods outlined in Tixier et al. (2003). Briefly, we used the GCSOLAR software to calculate a pseudo-first-order rate constant based on diclofenac's absorbance spectrum (Figure SI4) and its quantum yield previously determined by Davis et al. (2017) (i.e., 0.071). We calculated diclofenac's k_{photo} during spring and summer in the top first centimetre of a water body at conditions in Mainz, Germany (i.e., roughly the center of the Rhine river basin, latitude= 49.99 N, elevation= 89 m above sea level). For other compounds showing susceptibility towards phototransformation, we then multiplied the prior phototransformation rate constant for diclofenac with a factor describing the respective compound's rate constant relative to diclofenac's rate constant measured in our direct phototransformation experiments. Further details are provided in SI1.5.

2.4.2. Sorption experiments and prior estimation of K_{oc}

To gather consistently derived experimental K_{oc} values for the selected field compounds, we carried out a series of sorption experiments following the experimental procedures described by Davis and Janssen (2020) (further details in SI1.6). To that end, sorption experiments were carried out with both sediments used in modified OECD 308-type studies by Seller et al. (2021) and one standardized soil (i.e., LUFA 2.1), such that experiments captured sorption under two different pH conditions and with two different sediment TOC contents (Table SI4). Sorption experiments were carried out in two stages; first, we determined the time needed to reach sorption equilibrium, and second, we derived sorption isotherms for five concentration levels spanning two orders of magnitude of initial aqueous concentrations (i.e., 0.3 to 30 μg L^{-1}). According to outcomes of the first stage of sorption experiments, an equilibration time of 16 h was used to ensure steady conditions in all experimental vessels during the second stage of sorption experiments. Sorption isotherms were derived using a linear and a Freundlich model. However, data suggested that linear sorption isotherms were suitable to describe sorption behavior of most compounds. Therefore, we calculated K_{oc} values based on K_d values measured in each

of the sediments/ soil (OECD, 2000).

To derive K_{oc} prior distributions to describe sorption behavior of our compounds in the laboratory and in the field, experimentally determined K_{oc} values were averaged across the three sediments/ soil. In case of pesticides, which were only studied in the laboratory, prior estimates for K_{oc} values were based on data provided by the Pesticides Properties Database (PPDB) of the University of Hertfordshire. Prior distributions for K_{oc} were assumed to be lognormal due to the rather high variability of experimentally determined K_{oc} values and the fact that only positive values are meaningful for this quantity. Mean and standard deviation of the K_{oc} priors' lognormal distributions were derived from our own experimental K_{oc} values as described in SI1.6.

3. Results and discussion

3.1. Phototransformation and sorption experiments

3.1.1. Phototransformation kinetics and derivation of k_{photo} priors

Phototransformation experiments were run to identify compounds that might potentially undergo phototransformation reactions in the field, given an average hydraulic residence time in the Rhine river catchment of roughly 7 days (Honti et al., 2018a). We found that direct phototransformation could be a relevant removal pathway for five field compounds, i.e., diclofenac, hydrochlorothiazide, aliskiren, atazanavir, and sulfamethoxazole, with the first two compounds showing the most rapid transformation (Fig. 1). Those results are in line with previous studies showing the susceptibility of aliskiren, diclofenac, hydrochlorothiazide, and sulfamethoxazole towards direct phototransformation; especially the phototransformation behavior of diclofenac has been studied widely (Avetta et al., 2016; Davis et al., 2017; Gonçalves et al., 2021; Peuravuori 2012). To our knowledge, no previous studies examined phototransformation behavior of atazanavir. Our results indicate that this compound can indeed undergo direct phototransformation at conditions relevant for rivers and lakes, as it absorbs light within the solar spectrum (Figure SI4). Therefore, we considered phototransformation as additional dissipation process for those five compounds in the Rhine catchment model (see 3.3). Prior distributions of k_{photo} for model calibration were derived as described in 2.4.1 and are provided in Table SI6.

Indirect phototransformation appeared to be a less significant removal pathway for the selected field compounds. Compound

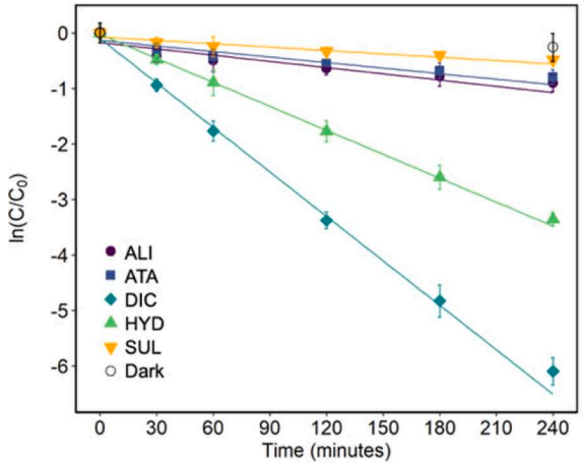

Fig. 1. Transformation kinetics of field compounds showing significant susceptibility towards direct phototransformation, i.e., aliskiren (ALI), atazanavir (ATA), diclofenac (DIC), hydrochlorothiazide (HYD), and sulfamethoxazole (SUL), in nanopure water buffered at pH= 8 under the solar simulator conditions. The plotted dark control represents the average concentration of the five compounds shown after 0 and 4 h of experiment.

dissipation during experiments targeting indirect phototransformation was statistically significant only for the four compounds carbamazepine, clopidogrel carboxylic acid, lidocaine, and mefenamic acid, with the latter showing the greatest susceptibility towards indirect phototransformation, which is in line with studies reported in the literature (Davis et al., 2017). However, it has to be noted that we did not detect removal via indirect phototransformation from the two natural waters tested, i.e., from the river and pond samples, but only from the test water amended with PLFA to a high DOC concentration of 10 mg L^{-1}. Even at this elevated DOC concentration, the maximum observed rate for indirect phototransformation was in all cases <0.067 d^{-1}. Based on the fact that DOC concentrations in the river Rhine are commonly 3–9 fold lower (Abril et al., 2002; Rodríguez-Murillo et al., 2015), and considering the compound's average hydraulic residence time within the Rhine river catchment (i.e., 7 days), we assume that indirect phototransformation is not a relevant dissipation process for the selected field compounds in this catchment and therefore neglect this transformation pathway in the Rhine catchment model.

3.1.2. Sorption behavior and derivation of K_{oc} priors

A compilation of measured K_d and K_{oc} values for selected field compounds is provided in Table 1. Field compounds covered a broad range of different sorption behavior with calculated K_d values ranging from <0.17 to 286 L kg^{-1} resulting in K_{oc} values ranging from 15 to 28′550 L kg^{-1}. Highest affinity for sorption to solids with K_{oc} values >1000 L kg^{-1} in at least one of the tested sediments/ soil were calculated for aliskiren, citalopram, fexofenadine, sitagliptin, trimethoprim, and venlafaxine, which is in line with previously reported experimentally determined K_{oc} values (Table 1 and Table SI19) (Barron et al., 2009; Klement et al., 2018; Le Guet et al. 2018; Li and Zhang 2017). K_{oc} values consistently <100 L kg^{-1} were determined for nine compounds, i.e., acesulfame, bezafibrate, cyclamate, irbesartan, levetiracetam, lidocaine, saccharin, sulfamethoxazole, and valsartan. Accordingly, previous studies on acesulfame and sulfamethoxazole report little sorption to soil, sludge, or sediment (Barron et al., 2009; Carballa et al., 2008; Le Guet et al. 2018; Storck et al., 2016). In case of bezafibrate, K_{oc} values reported in the literature are mostly higher than here determined K_{oc} values. However, those previous sorption studies were performed in soil with partially lower pH (i.e., pH= 3.5–6.4, Table SI18) than the here employed sediments/ soil (i.e., pH= 5–7.5) (Barron et al., 2009; Revitt et al., 2015). Due to the low pKa of bezafibrate (i.e., pKa= 3.83), the compound can be assumed to have been present in its deprotonated, anionic form in our own sorption experiments, while the lower pH in previous soil studies may have resulted in presence of more neutral species leading to increased sorption. For compounds exhibiting moderate sorption behavior, i.e., 5-methylbenzotriazole, atenolol, carbamazepine, diclofenac, lamotrigine, mefenamic acid, and metoprolol, our experimentally determined K_{oc} values mostly fall within the range previously reported in literature (Table 1). Based on our literature search (Table SI19), which we do not claim to be fully comprehensive, we concluded that experimentally derived K_{oc} values have not been reported previously for 13 of our test compounds (Table 1), highlighting the importance of performing our own sorption studies prior to estimating k'_{bio}.

Prior distributions for K_{oc} values used for calibration of the k'_{bio} model frameworks to determine $k'_{bio,field}$ and $k'_{bio,lab}$ (see 3.3 and 3.4) were derived as described in 2.4.2 and are listed in Table SI6. In this context, we acknowledge that the assumption behind using K_{oc} values to describe a compound's sorption behavior, i.e., that compounds predominantly sorb to organic carbon, is not necessarily correct for small polar or charged compounds, which might also sorb to minerals. Because more detailed studies on sorption mechanisms of our many field compounds were out of scope, we attempted to account for those variabilities in sorption behavior by defining prior distributions of K_{oc} based on average values derived from three sediments/soils differing in TOC, grain size distribution, and pH. In doing so, we try to describe a

Table 1
Experimentally determined K_d and K_{oc} values. R^2 indicates the goodness of the fit of the linear model to the experimental data, n.d. indicates that K_d and K_{oc} could not be determined due to bad fit of the linear model (i.e., R^2 <0.7), n.s. indicates that calculated K_d and K_{oc} values were negative as a result of very little/ no sorption. Based on our literature search, the column "Literature K_{oc} values" lists lowest and highest experimentally determined K_{oc} vales in sludge, soil, or sediment reported in the literature. Further details on literature K_{oc} values and references to the here provided values are given in Table SI19.

Compound	Sediment/ Soil	K_d [kg L^{-1}]	K_{oc} [kg L^{-1}]	R^2	Literature K_{oc} [kg L^{-1}]
5MB	LUFA 2.1	n.d.	n.d.	n.d.	39–110
	Pond	16.9 ±	169±4	0.99	
	River	0.4	113	0.99	
		0.9 ± 0.1	±12.5		
ACE	LUFA 2.1	n.s.	n.s.	n.s.	1.1–11.2
	Pond	2.3 ±	23±0.6	0.99	
	River	0.06	21±7	0.85	
		0.17			
		±0.06			
ALI	LUFA 2.1	29.6 ±	4169	0.99	Not available
	Pond	2.1	±295	0.95	
	River	35±2	350±20	0.97	
		32±2.5	4000		
			±312		
ATA	LUFA 2.1	3.3 ± 2	465	0.94	Not available
	Pond	24±2	±281	0.89	
	River	<0.17	240±20	0.73	
			<21		
ATE	LUFA 2.1	n.d.	n.d.	n.d.	63–5000
	Pond	7.8 ± 0.2	78±2	0.99	
	River	1.1 ± 0.2	140±20	0.93	
BEZ	LUFA 2.1	n.d.	n.d.	n.d.	54–568
	Pond	3.9 ± 0.2	39±2	0.97	
	River	n.s.	n.s.	n.s.	
BIC	LUFA 2.1	4 ± 1.7	563	0.71	Not available
	Pond	26±2	±239	0.87	
	River	n.s.	260±20	n.s.	
			n.s.		
CAR	LUFA 2.1	n.d.	n.d.	n.d.	8–2650
	Pond	6.36±1.7	64±17	0.81	
	River	3.31	473±56	0.97	
		±0.39			
CIT	LUFA 2.1	163±11	22957	0.85	6918–665,000
	Pond	286±10	±1549	0.97	
	River	230±60	2860	0.97	
			±100		
			28750		
			±7500		
CLO	LUFA 2.1	n.d.	n.d.	n.d.	Not available
	Pond	5.6 ± 0.2	56±2	0.97	
	River	0.8 ± 0.2	100±25	0.98	
CYC	LUFA 2.1	n.d.	n.d.	n.d.	Not available
	Pond	<0.62	<6.2	0.82	
	River	n.d.	n.d.	n.d.	
DIC	LUFA 2.1	n.d.	n.d.	n.d.	72 - 2630
	Pond	10.5 ±	105±3	0.99	
	River	0.3	187±18	0.99	
		1.5 ±			
		0.15			
FEX	LUFA 2.1	26±1	3661	0.96	1130–11,512
	Pond	37.8 ±	±140	0.99	
	River	0.7	378±7	0.98	
		14±1	1750		
			±125		
GAB	LUFA 2.1	1.5 ± 0.2	211±28	0.95	Not available
	Pond	6.8 ± 0.2	68±2	0.99	
	River	1 ± 0.1	125	0.92	
			±12.5		
HYD	LUFA 2.1	0.7 ± 0.1	99±14	0.86	Not available
	Pond	9.1 ± 0.2	91±2	0.99	
	River	0.7 ± 0.1	88±12.5	0.97	
IRB	LUFA 2.1	n.d.	n.d.	n.d.	74 - 2298
	Pond	6.5 ± 0.3	65±3	0.96	
	River	n.s.	n.s.	n.s.	
LAM	LUFA 2.1	2.8 ± 0.4	394±56	0.76	93 - 703
	Pond	22.4 ±	224±5	0.99	
	River	0.5	213±19	0.99	
		1.7 ±			
		0.15			
LEV	LUFA 2.1	0.42	59±8.4	0.92	Not available
	Pond	±0.06	41±13	0.86	
	River	4.1 ± 1.3	55±8.7	0.95	
		0.44			
		±0.07			
LID	LUFA 2.1	0.55+0.1	77±14	0.88	51 - 80
	Pond	7.9 ± 1.1	79±11	0.97	
	River	0.53	66±10	0.89	
		±0.08			
MEF	LUFA 2.1	25±6	3521	0.99	52 - 27,000
	Pond	38±1.6	±845	0.96	
	River	2 ± 1	380±16	0.97	
			250		
			±140		
MET	LUFA 2.1	0.6 ± 0.1	90±20	0.79	58 - 3157
	Pond	12.6 ±	114±2	0.99	
	River	0.2	250	0.97	
		2 ± 0.1	±12.5		
SAC	LUFA 2.1	n.s.	n.s.	n.s.	Not available
	Pond	n.d.	n.d.	n.d.	
	River	n.s.	n.s.	n.s.	
SIT	LUFA 2.1	56±1.9	7887	0.98	Not available
	Pond	59±2	±267	0.97	
	River	20±1.7	590±20	0.98	
			2500		
			±212		
SUL	LUFA 2.1	n.d.	n.d.	n.d.	11 - 3802
	Pond	1.7 ± 0.1	17±1	0.98	
	River	n.d.	n.d.	n.d.	
TRI	LUFA 2.1	10.6 ±	1493	0.97	264 - 4533
	Pond	4.4	±619	0.97	
	River	97±4	970±40	n.d.	
		n.d.	n.d.		
VAL	LUFA 2.1	n.d.	n.d.	n.d.	Not available
	Pond	4.4 ± 0.1	44±1	0.99	
	River	n.d.	n.d.	n.d.	
VEN	LUFA 2.1	37.7 ± 1	5309	0.97	Not available
	Pond	29±1	±140	0.97	
	River	25±2	290±10	0.94	
			3125		
			±250		

reasonable range of sorption behavior a compound might exhibit when exposed to different environmental conditions and sediments along the Rhine river catchment.

3.2. Compound concentrations and loads in the Rhine river basin

All of our 27 field compounds were detected in water samples from the SMPC sampling locations during both campaigns P1 and P3, with 21 and 17 compounds detected at each sampling location at concentrations above their limits of quantification (LOQs, Table SI10-Table SI13) during P1 and P3, respectively, indicating continuous use and emissions in significant amounts of those compounds. Measured compound concentrations are given in Tables SI10–SI13. Depending on compound and sampling location, concentrations ranged from <1 ng L^{-1} to ≥5 μg L^{-1} during P1 and from <1 ng L^{-1} to ≥2.5 μg L^{-1} during P3, which is comparable to the concentration range previously measured for various pharmaceuticals or artificial sweeteners in water samples from the river Rhine (Ruff et al., 2015). Generally, highest compound concentrations were measured in samples taken from two of the Rhine's tributaries, i.e., Schwarzbach and Emscher, which enter the main channel of the Rhine at 475 and 798 Rhine km, respectively. At all sampling locations, 4/5-methylbenzotriazole and acesulfame, together with gabapentin during P1 and cyclamate during P3, were measured at highest

concentrations (Fig. 2).

The weekly loads of compounds along the Rhine and its tributaries were calculated separately for the P1 and P3 campaigns by multiplying corresponding discharge and concentration measurements at each location (discharge measurements in Table SI10-Table SI13). Generally, compound loads gradually increased along the Rhine during both sampling campaigns (Fig. 2) as the Rhine receives input from tributaries and WWTPs distributed all along the river. The cumulative weekly loads of our field compounds passing the last monitoring station before the Rhine estuary (i.e., Lobith at 865 Rhine km) were 2.5 and 1.6 tons during P1 and P3, respectively (Fig. 2). Quarterly consumption of the majority of the field compounds in Germany and Switzerland can be assumed to have been similar during the P1 and P3 campaign (Table SI8), hence the reduced cumulative compound loads in P3 point towards increased compound transformation during summer months. While compound removal in WWTPs can potentially undergo seasonal changes (Di Marcantonio et al. 2020; Fernández et al., 2014; Kahl et al., 2018; Varga et al. (2023) did not find a statistically significant seasonal dependency of the field compounds' emission into the Rhine based on WWTP effluent monitoring data, except for three compounds (ACE, CYC, and GAB). Hence, we assume that at least part of the almost 40% decrease in cumulative compound load along the Rhine during P3 resulted from more rapid transformation within the riverine environment. Such an increase in compound removal from the aquatic environment during summer can, amongst others, result from increased biotransformation due to higher microbial biomass and/ or activity at elevated water temperatures (Table SI16), greater abundance of phototrophic degrader bacteria, as well as from increased removal of photo-reactive compounds at higher light intensities and longer light exposure times.

3.3. Biotransformation in the Rhine river basin - calculation of $k'_{bio,field}$ values

We calculated $k'_{bio,field}$ values to describe the compounds' biotransformation potential in the Rhine catchment. Compound loads measured along the Rhine and its tributaries, as well as laboratory-derived sorption and phototransformation parameters served as basis for model calibration. The Rhine catchment model generally achieved good fits to the compound loads monitored during both field campaigns (Figs. 3B and SI7). Calibrated $k'_{bio,field}$ values are listed in Tables SI14 and SI15 and posterior distributions are shown in Fig. 3A. Mean $k'_{bio,field}$ values ranged from <1 to >3000 L (g OC d)$^{-1}$ (Fig. 3A). It has to be noted that the model framework only allows to differentiate $k'_{bio,field}$ values <30 to >1000 L (g OC d)$^{-1}$; lower $k'_{bio,field}$ values practically mean that no transformation was observed along the Rhine, higher $k'_{bio,field}$ values indicate complete disappearance of the respective compound between subsequent sampling locations.

Based on the differences in compound loads accumulating along the Rhine during the two field campaigns, biotransformation can be assumed to have been increased during P3 compared to P1 (see 3.2). Accordingly, for eleven compounds (i.e., acesulfame, aliskiren, bezafibrate, diclofenac, levetiracetam, mefenamic acid, saccharin, sitagliptin, trimethoprim, valsartan, and venlafaxine), $k'_{bio,field}$ values derived from P3 data ($k'_{bio,field,P3}$) were significantly higher than $k'_{bio,field}$ values derived from P1 data ($k'_{bio,field,P1}$), i.e., there was no overlap of their interquartile range. Another group of eight compounds showed a possible but less significant difference of the same kind (i.e., atazanavir, atenolol, bicalutamide, citalopram, cyclamate, lidocaine, metoprolol, and saccharin). For clopidogrel carboxylic acid, hydrochlorothiazide, lamotrigine, and sulfamethoxazole, $k'_{bio,field}$ values were similar during P1 and P3, suggesting that their biotransformation is less sensitive towards temporal variations, e.g., changes in season. Carbamazepine and fexofenadine were the only counter-examples with significantly higher $k'_{bio,field,P1}$ values compared to $k'_{bio,field,P3}$ values (i.e., no overlap of interquartile range); however, mean $k'_{bio,field}$ values derived for carbamazepine were close to/below the here defined identifiability range. In the case of fexofenadine, an antihistamine, quarterly consumption data available to estimate compound emission into the Rhine may not fully capture the seasonal use of this pharmaceutical, potentially resulting in overestimation of both emissions and $k'_{bio,field,P1}$.

It can be assumed that a major factor driving differences between $k'_{bio,field,P1}$ and $k'_{bio,field,P3}$ are seasonal variations in water temperature (Table SI16). Ideally, the Rhine catchment model should be updated to account for the compounds' varying transformation kinetics at changing temperatures. However, a simple correction of $k'_{bio,field}$ according to the Arrhenius equation does not seem feasible as the ratios between $k'_{bio,field,P1}$ and $k'_{bio,field,P3}$ vary across compounds, i.e., there is no systematic increase for all compounds' removal via biotransformation during summer (Fig. 3A). This is in line with recent findings of (Meynet et al., 2020) showing that temperature optima for micropollutant biotransformation in activated sludge can vary strongly depending on compound and expected reaction pathways.

Generally, absolute $k'_{bio,field}$ values are to be treated with caution as our model framework calculates (bio)transformation for an entire catchment, which requires a number of simplifying assumptions resulting in uncertainties in model output parameters. It is not possible

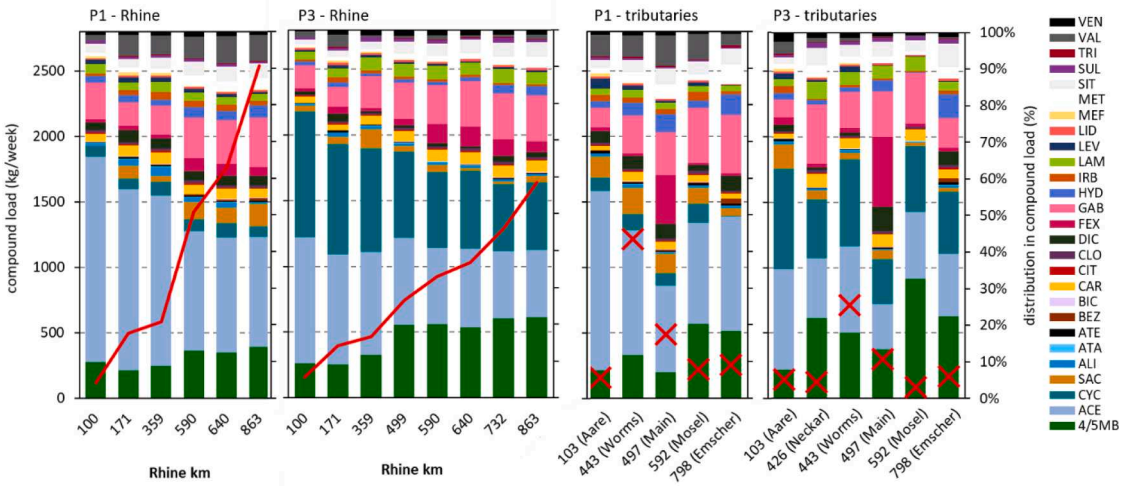

Fig. 2. Field compounds' relative abundances and loads along the main channel of the river Rhine and its major tributaries measured during the P1 and P3 campaigns. Total compound loads determined along the main channel of the Rhine are shown as red line, compound loads in the Rhine's tributaries are shown as red crosses. The color-coded bar charts indicate contribution of each compound to the total compound load (see compound name abbreviations in Table SI1).

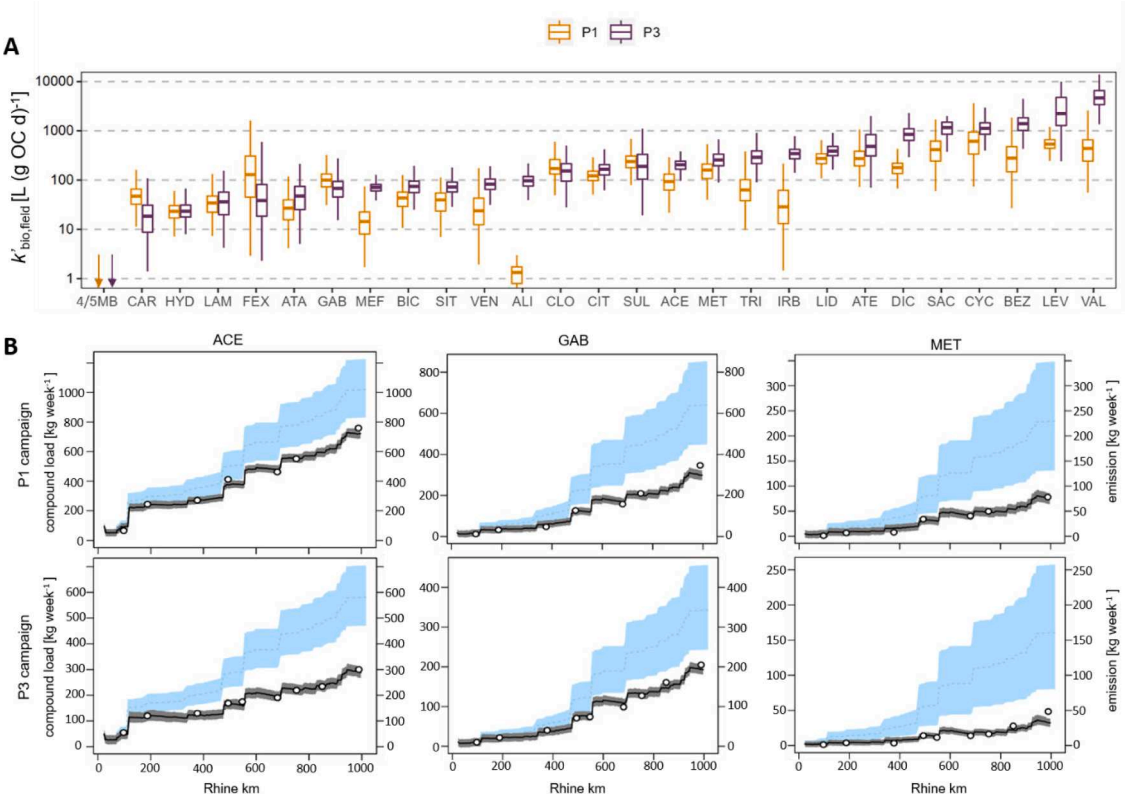

Fig. 3. Biotransformation kinetics and loads in the Rhine river catchment during spring (P1 campaign) and summer (P3 campaign) 2017. (A) $k'_{bio,field}$ posteriors when fitting the Rhine catchment model to compound loads measured along the Rhine during P1 and P3. (B) Model fits (black line) and 95% confidence intervals (gray bands around inferred compound load) to compound loads measured along the Rhine (dots). Estimated compound emissions into the Rhine (secondary y-axis) are shown as dotted line with its uncertainties range plotted in light blue. Differences between estimated emission and measured/ modelled compound load suggest compound removal from the Rhine river catchment. Please note that first and secondary y-axis are plotted on different scales for each compound. Compound name abbreviations are given in Table SI1.

to distinguish between biotransformation and other fate processes based on observed compound loads in the Rhine water body exclusively. Hence, $k'_{bio,field}$ values are conditional on the assumptions made during model calibration. For example, by using a single K_{oc} value for the entire catchment, the model framework cannot capture spatially varying sorption behavior of compounds under changing bed sediment and suspended particle properties within the stream network. As indicated by variable outcomes of our sorption experiments and the literature data, such variability is undeniable (Table 1). Yet, the posterior distributions of k_{hyro}, k_{photo}, and K_{oc} closely followed their prior distributions, which indicates that there was no strong evidence against our laboratory experiments-based prior assumptions in the observed field data. However, as expected, prior distributions for abiotic transformation influenced calibrated $k'_{bio,field}$ values. This is especially critical in the case of phototransformation, as translating k_{photo} from laboratory to field is subject to a number of uncertainties, e.g., actual light penetration into the water body. Sensitivity to this parameter was nonlinear, i.e., changing the mean prior value of k_{photo} by a factor of 2 did not result in statistically significant changes of the $k'_{bio,field}$ estimates, however, 5-fold changes of k_{photo} resulted in $k'_{bio,field}$ estimates differing by two orders of magnitude. However, previous field studies on phototransformation kinetics of diclofenac at the surface of German river stretches (<15 cm water depth) during the month of July resulted in rate constants differing by a factor of ≤2.4 compared to the here employed mean of the k_{photo} prior distribution, supporting its feasibility for calibration of the Rhine catchment model (Kunkel and Radke 2012; Radke et al., 2010). Finally, from a microbiology perspective, the model would need to be further underpinned with molecular biology data characterizing the potential of sediment and water microbial communities to catalyze a range of initial contaminant biotransformation reactions. Consequently, the parameters of the Rhine model should be considered as abstract values that describe the observed behavior at the catchment scale, and $k'_{bio,field}$ estimates should not be considered measurable as such at any specific location in the catchment.

Yet, when including data from our phototransformation and sorption experiments, the Rhine catchment model allowed to, at least semi-quantitatively, elucidate biotransformation kinetics of >20 chemical contaminants ubiquitously present within the river Rhine. It can therefore be considered a valuable contribution towards estimating the rate and extent of biotransformation processes in riverine environments, even when WWTPs densely distributed along the river preclude the direct observation of compound attenuation. While $k'_{bio,field,P1}$ and $k'_{bio,field,P3}$ differ in terms of their absolute values, the compounds' rank relative to each other was well conserved (Spearman rank $\rho = 0.78$, p-value <0.05) meaning that the Rhine catchment model identified the same compounds as slowly or rapidly degrading regardless of whether calibrated with P1 or P3 data. Therewith, outcomes of the Rhine catchment model qualitatively align well with findings of previous biotransformation studies in laboratory or field. For example, smallest $k'_{bio,field}$ values during both field campaigns were calculated for carbamazepine and 4/5-methylbenzotriazole. Carbamazepine is well known to remain persistent in aquatic environments (Coll et al., 2020; Tixier et al., 2003). While 5-methylbenzotriazole was previously shown to biotransform at moderate rates in water-sediment systems (Seller et al., 2021), the low $k'_{bio,field}$ values are probably distorted by the persistent 4-methylbezotriazole, which cannot be distinguished from 5-methylbenzotriazole with the analytical method used here (Dummer 2014). Highest $k'_{bio,field}$ values were found for compounds easily biodegraded by a range of enzymes present in WWTP effluent impacted surface waters or widespread among aquatic microbial communities in general, e.

g., atenolol, bezafibrate, levetiracetam, or valsartan (Achermann et al., 2018; Desiante et al., 2021; Seller et al., 2021).

3.4. Biotransformation in laboratory studies - calculation of $k'_{bio,lab}$ values

The $k'_{bio,lab}$ values were calculated based on data from modified OECD 308-type studies in order to enable a comparison of laboratory- and field derived transformation kinetics. Further, $k'_{bio,lab}$ values were derived from studies conducted with different inocula, allowing to simultaneously test whether the k'_{bio}-concept could facilitate unifying observations from different laboratory studies as previously suggested, yet only tested on three compounds (Honti et al., 2016). Hence, we inferred $k'_{bio,lab}$ from experiments conducted in river and pond inoculum individually ($k'_{bio,lab,r}$ and $k'_{bio,lab,p}$, respectively) and across both experimental setups ($k'_{bio,lab,joint}$) for 38 compounds. First, $k'_{bio,lab}$ values were normalized to TOC as proxy for degrader biomass and ranged from 0.004 to >4000 L (g OC d)$^{-1}$ with standard model errors mostly below 10% (Fig. 4, Table SI16). It has to be noted that $k'_{bio,lab}$ values <0.01 or >100 L (g OC d)$^{-1}$ are subject to identifiability issues due to slow or very fast transformation, respectively.

Comparison of mean $k'_{bio,lab,r}$ to mean $k'_{bio,lab,p}$ revealed that the two quantities show a statistically significant, strong correlation (i.e., Pearson's $r = 0.81$, p-values <0.001, Figure SI8), regardless of slight differences in absolute values. Further, it was possible to derive biotransformation rate constants that are valid across both sets of biotransformation simulation studies ($k'_{bio,lab,joint}$, Fig. 4A). The good fit to the experimental data when jointly fitting data from both experiments (Figs. 4B and SI9) confirms the hypothesis that the k'_{bio}-concept allows linking biotransformation kinetics of compounds with a range of different properties across different water-sediment studies. Comparing the individual fits to the joint fit revealed that the joint model solution yielded more likely results for all compounds except for atenolol and fenoxycarb, whose $k'_{bio,lab,r}$ values were outside of the here defined identifiability range (comparison based on Akaike Information Criterion, Table SI17). Further, for the large majority of compounds, $k'_{bio,lab,joint}$ values were less uncertain than values from individual fits (coefficients of variation (CV) in Table SI17).

Second, in addition to TOC normalization, we also derived $k'_{bio,lab}$ values normalized to what we assume to be a more precise measure of

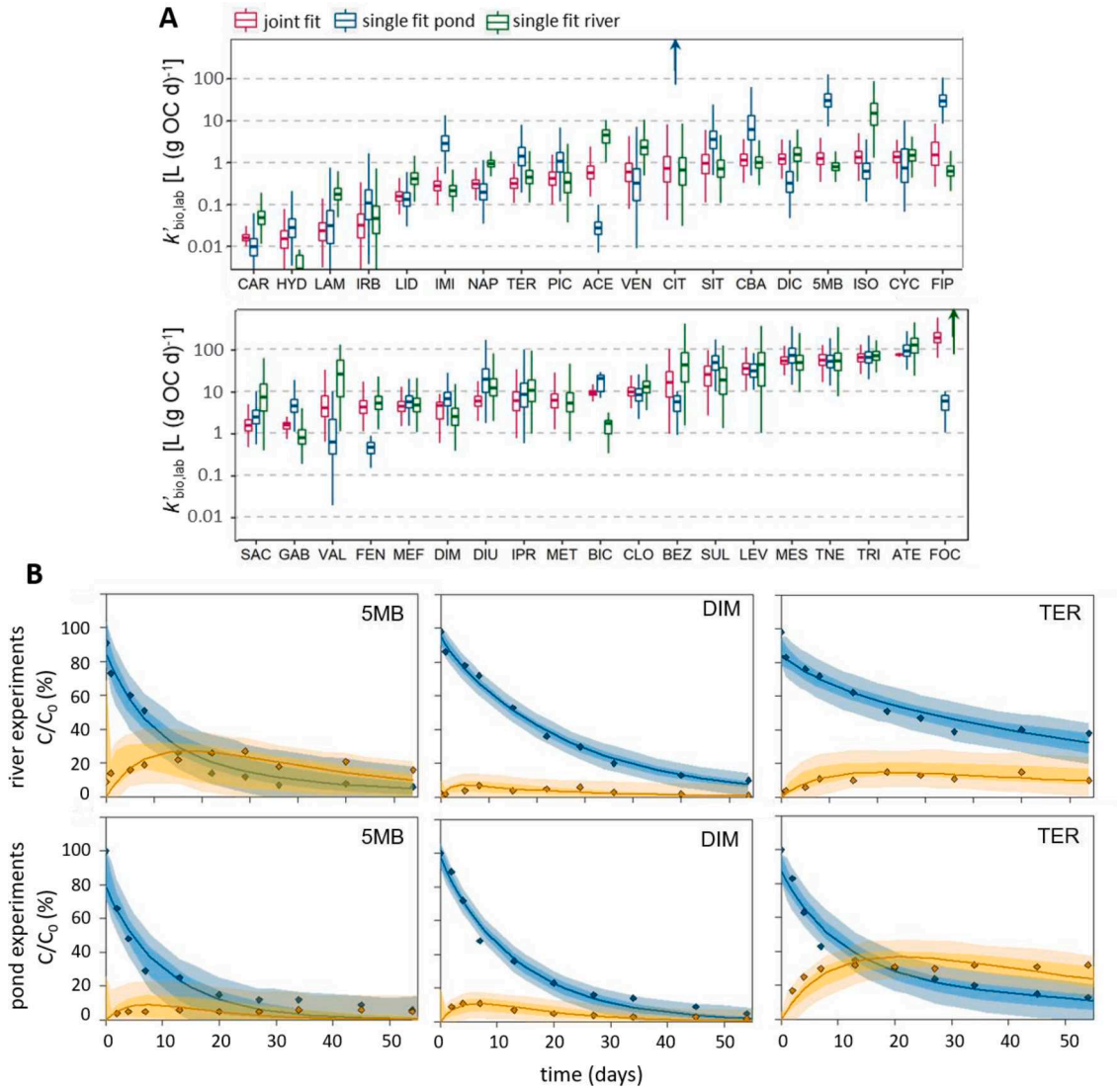

Fig. 4. Biotransformation kinetics in modified OECD 308-type studies. (A) $k'_{bio,lab}$ posterior distributions when fitting the k'_{bio}-model framework to river and pond experiments individually and jointly across both experiments ($k'_{bio,lab,joint}$). (B) Model fits (lines) to data measured in modified OECD 308-type experiments (diamonds) when using $k'_{bio,lab,joint}$ to describe biotransformation kinetics in experiments conducted with pond and river inoculum, respectively. Blue and yellow data traces show compound mass residues in water column and sediment layer of the experimental vessels, respectively. Opaque shaded areas indicate confidence regions of parametric uncertainty, more transparent areas indicate total uncertainty including random measurement errors. See compound name abbreviations in Table SI1.

total biomass than TOC, i.e., cell densities measured using flow cytometry during modified OECD 308-type studies. Those $k'_{bio,lab,cell}$ values ranged from 0.01 to >4000 mL (10^9 cells d)$^{-1}$ (Table SI18) and, when inferred from river and pond experiments individually, correlated equally strongly as $k'_{bio,lab}$ values normalized to TOC (i.e., Pearson's r = 0.81, p-value< 0.001, Fig. SI8). Yet, t-statistics on the correlation between cell density-normalised $k'_{bio,lab,cell,r}$ and $k'_{bio,lab,cell,p}$ showed that the slope of the linear regression was not statistically significantly different from 1, while, in contrast, the correlation between the two quantities normalized to TOC had a slope distinctly lower than 1 (Fig. SI8). Those differences in slope indicate that normalization to cell densities as a more precise measure for total biomass increases the transferability of $k'_{bio,lab}$ between different experiments.

In a regulatory context, in which OECD biotransformation studies are typically performed, model frameworks that enable system-agnostic approaches are of special interest in risk assessment of synthetic chemicals where compound-specific transformation parameters are prime targets. As the measurement of biodegradation kinetics according to regulatory testing guidelines is laborious and costly, reducing the amount of experiments that need to be performed in order to determine a compound's biotransformation potential brings economic and ecological benefits allowing to more easily consider a compound's environmental degradability during earlier phases of chemical design (Fenner et al., 2020). In the future, different indicators for degrader biomass, such as ATP measurements, could be tested to further improve the transferability of kinetic parameters between different studies.

3.5. Comparison of biotransformation kinetics in modified OECD 308-type studies and the Rhine river basin

3.5.1. Direct comparison of $k'_{bio,lab}$ and $k'_{bio,field}$

We compared $k'_{bio,lab}$ and $k'_{bio,field}$ values in order to assess to what extent biotransformation data from laboratory experiments reflect compound degradation in the Rhine river basin. Comparing biotransformation between laboratory and field was possible for 23 compounds, i.e., field compounds for which we were able to derive both meaningful $k'_{bio,field}$ and $k'_{bio,lab,joint}$ values. We directly compared $k'_{bio,field,P3}$ to $k'_{bio,lab,joint}$ estimates as the temperatures measured in the water column of the main channel of the Rhine during P3 (Table SI16) were in the same range as temperatures during modified OECD 308-type studies, i.e., 22±2 °C (Seller et al., 2021). On the laboratory side, we used $k'_{bio,lab,joint}$ values normalized to TOC to allow for a direct comparison of quantities.

Comparing absolute values of $k'_{bio,field,P3}$ to $k'_{bio,lab,joint}$ revealed that $k'_{bio,lab,joint}$ values are generally about two orders of magnitude lower than $k'_{bio,field,P3}$ values (Fig. 5A). While uncertainties associated with absolute values of $k'_{bio,field,P3}$ are to be expected (see 3.3), the large difference between laboratory and field k'_{bio} may point to a systematic under-estimation of field degradation rates by laboratory simulation tests. Faster transformation in the field can be speculated to be due to the fact that the compounds were exposed to more diverse microbial degraders and degradation pathways during their travel in the Rhine river catchment than while being entrapped in experimental vessels (Chalifour et al., 2021). In its current form (i.e., using TOC as proxy for

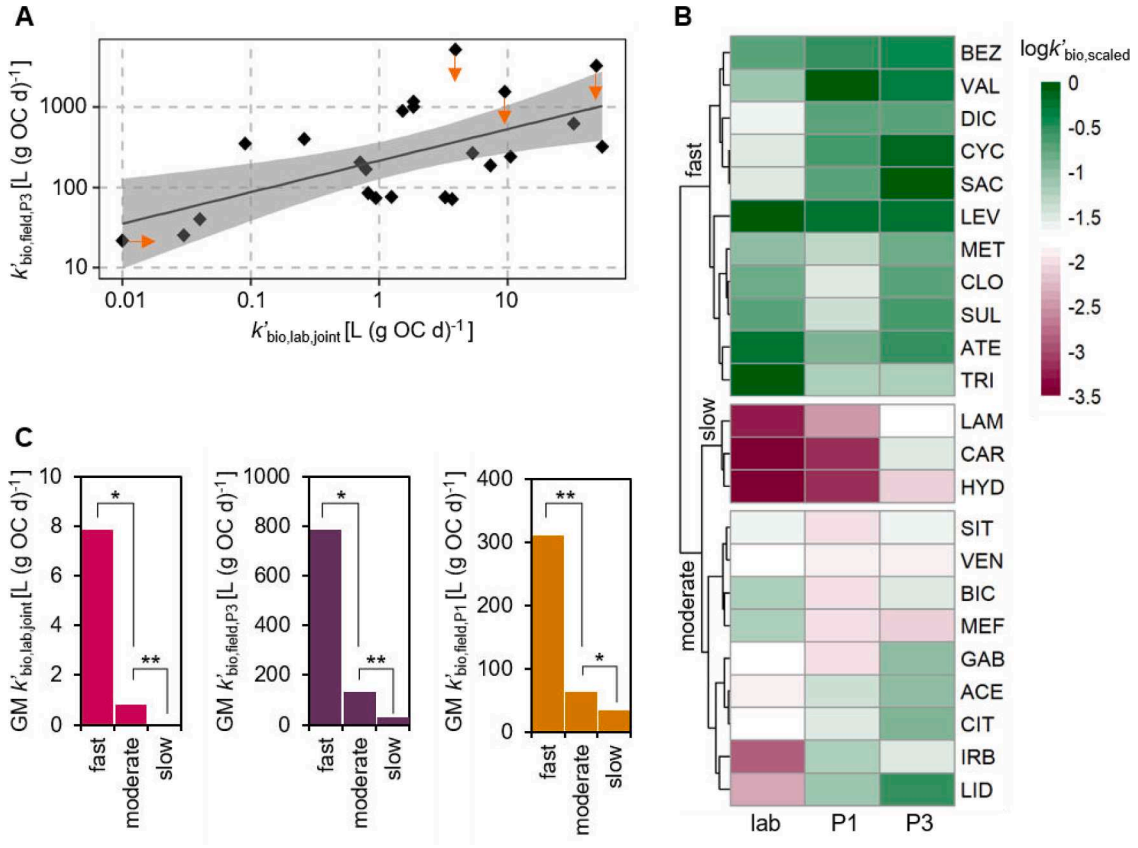

Fig. 5. Comparison of $k'_{bio,lab,joint}$ and $k'_{bio,field}$ values. (A) Correlation between $k'_{bio,lab,joint}$ and $k'_{bio,field,P3}$. Pearson's r = 0.6, p-value<0.05. Arrows indicate compounds outside the here defined identifiability range, i.e., 30 L (g OC d)$^{-1}$ ≤ $k'_{bio,field,P3}$ ≤ 1000 L (g OC d)$^{-1}$ and 0.01 L (g OC d)$^{-1}$ ≤ $k'_{bio,lab,joint}$ ≤ 100 L (g OC d)$^{-1}$. (B) Clustered heatmap showing $k'_{bio,lab,joint}$, $k'_{bio,field,P1}$, and $k'_{bio,field,P3}$ values scaled to the range covered by the respective k'_{bio} values and then logarithmized to more clearly distinguish between lower values. The three clusters indicate compound groups showing slow (middle cluster), moderate (bottom cluster) and fast (top cluster) transformation relative to the other compounds investigated. (C) Geometric means (GM) of absolute k'_{bio} values calculated for the compounds in each group of the clustered heatmap, i.e., the compounds falling into the slow, moderate, and fast transformed group, respectively. T-tests were performed to determine statistical significance of the differences between GM k'_{bio} values; i.e., p-value < 0.05 (*), and p-value < 0.01 (**).

degrader biomass), the k'_{bio}-concept cannot account for such differing characteristics of microbial communities and their varying capacities for biotransformation of chemicals. Further, the extent of hyporheic exchange, i.e., contact with sediment biofilms, has been demonstrated to influence contaminant transformation (Jaeger et al., 2019; Jaeger et al., 2021). The lower $k'_{bio,lab,joint}$ values may suggest that even modified OECD 308-type test systems do not fully capture the impact of hyporheic exchange on biotransformation. Differences in sediment-water mixing might thus explain part of the increased degradation observed in the field.

Regardless of the differences in absolute values, linear regression revealed a statistically significant, moderate correlation between $k'_{bio,field,P3}$ and $k'_{bio,lab,joint}$ (i.e., Pearson's $r = 0.6$, p-value <0.05, Fig. 5A). The compound valsartan is the strongest outlier in the correlation between $k'_{bio,field,P3}$ and $k'_{bio,lab,joint}$. However, together with bezafibrate and levetiracetam, its $k'_{bio,field,P3}$ value is above the here defined identifiability range. Yet, it has to be noted that fixing outlier k'_{bio} values to the identifiability range (i.e., 30 L (g OC d)$^{-1} \leq k'_{bio,field,P3} \leq$ 1000 L (g OC d)$^{-1}$ and 0.01 L (g OC d)$^{-1} \leq k'_{bio,lab,joint} \leq$ 100 L (g OC d)$^{-1}$) does not influence correlation parameters, i.e., Pearson's r value of 0.6 remains.

Compared to previous – for the majority inconclusive – attempts to relate biotransformation parameters derived from standard OECD 308 studies (i.e., DT_{50}) to compound dissipation from riverine environments (Radke and Maier, 2014a), the observed relationship between $k'_{bio,lab}$ and $k'_{bio,field}$ values represents a clear improvement, suggesting that outcomes of laboratory simulation studies indeed – to some extent – reflect transformation kinetics observed in the environment. Hence, compared to DT_{50}, the k'_{bio}-concept appears more suitable to investigate biotransformation kinetics of compounds covering a wide range of different transformation and sorption behavior (e.g., field compounds with K_{oc} values covering roughly four orders of magnitude, Table 1) under spatially varying conditions. As indicated by the increased transferability of $k'_{bio,lab}$ values between different laboratory studies when normalized to cell densities (Figure SI8), a more accurate estimator of degrader biomass may allow to further converge $k'_{bio,lab}$ and $k'_{bio,field}$ values. While data on bacterial cell densities in the Rhine river catchment is not yet available, flow cytometry has been shown to be feasible for in-situ monitoring of cell densities in aquatic ecosystems (Besmer et al., 2014) and may hopefully be considered in future field campaigns.

3.4.2. *Relative ranking and clustering of compounds in laboratory and field*

Relative comparison of biotransformation kinetics in laboratory and field allowed a ranking-like analysis of the compounds. Derived k'_{bio} values were scaled to the range of values derived from laboratory studies, P1, and P3, respectively, and logarithmized to allow for a clear differentiation between lower values (Fig. 5B). Scaled k'_{bio} values differed $\leq$1 log unit between laboratory and field for the majority of compounds compared (i.e., 20 out of 23). Only for the three compounds carbamazepine, lamotrigine, and lidocaine scaled k'_{bio} values differed by 2 log units between laboratory and field. In case of carbamazepine, absolute $k'_{bio,lab,joint}$ and $k'_{bio,field,P3}$ values are lower than the here defined identifiability ranges and differences in scaled values are therefore to be treated with caution. The overall good accordance of scaled k'_{bio} vales indicates that, regardless of differences in absolute k'_{bio} values, the behavior of the field compounds relative to each other stays well conserved when relating outcomes of laboratory studies to biotransformation kinetics in the field.

Based on relative rankings, it was possible to cluster compounds into groups showing consistently fast, moderate, or slow transformation in both modified OECD 308-type studies and in the Rhine river catchment (Fig. 5B, C). Eleven compounds were identified as showing rather fast biotransformation in both laboratory and field studies, i.e., atenolol, bezafibrate, clopidogrel carboxylic acid, cyclamate, diclofenac, levetiracetam, metoprolol, saccharin, sulfamethoxazole, trimethoprim, and valsartan. The nine compounds acesulfame, bicalutamide, citalopram, gabapentin, irbesartan, lidocaine, mefenamic acid, sitagliptin, and venlafaxine showed moderate transformation kinetics. Finally, very slow to no biotransformation was observed in case of carbamazepine, hydrochlorothiazide, and lamotrigine. Based on this grouping into slow, moderate and fast degrading compounds, we calculated the geometric mean k'_{bio} values across all compounds belonging to the same group (Fig. 5C) from their absolute k'_{bio} values. Regardless whether considering field or laboratory data, mean k'_{bio} values differed significantly between each group allowing to clearly distinguish between compounds exhibiting different potential for biotransformation.

As our selected field compounds cover quite a wide range of different transformation and sorption behavior, here derived mean k'_{bio} values may be considered as points of reference when aiming to classify further compounds' potential for biotransformation based on field or laboratory data. Additional data from future laboratory and field studies could help to fine-tune mean $k'_{bio,lab}$/ $k'_{bio,field}$ values as points of reference both in terms of their feasibility for read-across applications between other laboratory and field studies and also in terms of their chemical applicability domain.

4. Conclusion

- We demonstrate that inverse modeling in combination with the k'_{bio}-concept can be used to describe biotransformation kinetics of WWTP effluent-borne compounds within a large, densely populated river basin. Our field studies reveal that the 27 field compounds are ubiquitously present within the Rhine river catchment and accumulate along the main channel of the Rhine, making it impossible to directly observe compound dissipation from monitoring data. Yet, $k'_{bio,field}$ showed to be a suitable parameter to at least semi-quantitatively elucidate the compounds' varying potential for biotransformation.
- The evaluation of aerobic laboratory simulation experiments proved that the k'_{bio}-concept allows to unify observed transformation kinetics across laboratory studies with different sediments (i.e., $k'_{bio,lab,joint}$), and that transferability of k'_{bio} between different water-sediment systems increases with a more precise measure of total biomass, i.e., employing bacterial cell densities rather than TOC as the normalizing factor for transformation.
- Comparing $k'_{bio,lab}$ and $k'_{bio,field}$ revealed that absolute values differed between laboratory and field, pointing towards faster transformation in the Rhine river basin. Yet, data gathered for the large number of 23 directly comparable compounds demonstrate that grouping based on relative compound behavior bears considerable potential when aiming to reflect biotransformation of micropollutants in natural riverine environments by performing biotransformation simulation studies.

Declaration of Competing Interest

The authors declare that they have no known competing financial interests or personal relationships that could have appeared to influence the work reported in this paper.

Data availability

Data will be made available on request.

Acknowledgements

We thank the International Commission for the Protection of the River Rhine (IKSR) for providing samples from the campaign "Sondermessprogramm Chemie 2017″ (SMPC). We further extend our thanks to Christian Stamm (Eawag) for fruitful discussions.

Funding

This work was supported by the German Federal Ministry for the Environment, Nature Conservation and Nuclear Safety (PIdent-2, FKZ 3717 65 409 0).

Supplementary materials

Supplementary material associated with this article can be found, in the online version, at doi:10.1016/j.watres.2023.119908.

References

Abril, G., Nogueira, M., Etcheber, H., Cabeçadas, G., Lemaire, E., Brogueira, M.J., 2002. Behaviour of organic carbon in nine contrasting European estuaries. Estuar. Coast. Shelf Sci. 54 (2), 241–262.

Achermann, S., Falås, P., Joss, A., Mansfeldt, C.B., Men, Y., Vogler, B., Fenner, K., 2018. Trends in Micropollutant Biotransformation along a solids retention time gradient. Environ. Sci. Technol. 52 (20), 11601–11611.

Adriaanse, P., Allen, R., Gouy, V., Hollis, J., Hosang, J., Jarvis, N., Jarvis, T., Klein, M., Layton, R., Linders, J., 1997. Surface water models and EU registration of plant protection products, p. 231. https://esdac.jrc.ec.europa.eu/public_path/projects_data/focus/docs/sw_en_6476VI96_24Feb1997.pdf.

Avetta, P., Fabbri, D., Minella, M., Brigante, M., Maurino, V., Minero, C., Pazzi, M., Vione, D, 2016. Assessing the phototransformation of diclofenac, clofibric acid and naproxen in surface waters: model predictions and comparison with field data. Water Res. 105, 383–394.

Barron, L., Havel, J., Purcell, M., Szpak, M., Kelleher, B., Paull, B., 2009. Predicting sorption of pharmaceuticals and personal care products onto soil and digested sludge using artificial neural networks. Analyst 134 (4), 663–670.

Batuik, R., Bergstrom, P., Kemp, M., Koch, E., Murray, L., Stevenson, J., Bartleson, R., Carter, V., Rybicki, N., Landwehr, J., Gallegos, C., Karrh, L., Naylor, M., Wilcox, D., Moore, K., Ailstock, M., Teichberg, M.. Chesapeake bay submerged aquatic vegetation water quality and habitat-based requirements and restoration targets: a second technical synthesis a watershed partnership. https://d18lev1ok5leia.cloudfront.net/chesapeakebay/documents/Submerged_Aquatic_Vegetation_Water_Qaulity_and_Habitat-Based_Requirements_and_Restoration_Targets_2000.pdf.

Berkner, S., Thierbach, C., 2014. Biodegradability and transformation of human pharmaceutical active ingredients in environmentally relevant test systems. Environ. Sci. Pollut. Res. 21 (16), 9461–9467.

Besmer, M.D., Weissbrodt, D.G., Kratochvil, B.E., Sigrist, J.A., Weyland, M.S., Hammes, F., 2014. The feasibility of automated online flow cytometry for in-situ monitoring of microbial dynamics in aquatic ecosystems. Front. Microbiol. 5, 265.

Brown, R., 1984. Relationships between suspended solids, turbidity, light attenuation, and algal productivity. Lake Reservoir Manage. 1 (1).

Carballa, M., Fink, G., Omil, F., Lema, J.M., Ternes, T., 2008. Determination of the solid–water distribution coefficient (Kd) for pharmaceuticals, estrogens and musk fragrances in digested sludge. Water Res. 42 (1), 287–295.

Chalifour, A., Walser, J.-C., Pomati, F., Fenner, K., 2021. Temperature, phytoplankton density and bacteria diversity drive the biotransformation of micropollutants in a lake ecosystem. Water Res. 202, 117412.

Coll, C., Bier, R., Li, Z., Langenheder, S., Gorokhova, E., Sobek, A., 2020. Association between aquatic micropollutant dissipation and river sediment bacterial communities. Environ. Sci. Technol. 54 (22), 14380–14392.

Cousins, I., Ng, C., Wang, Z., Scheringer, M., 2019. Why is high persistence alone a major cause of concern? Environ. Sci. Process. Impacts 21 (5), 781–792.

Davis, C.A., Erickson, P.R., McNeill, K., Janssen, E.M.L., 2017. Environmental photochemistry of fenamate NSAIDs and their radical intermediates. Environ. Sci. Process. Impacts 19 (5), 656–665.

Davis, C.A., Janssen, E.M.L., 2020. Environmental fate processes of antimicrobial peptides daptomycin, bacitracins, and polymyxins. Environ. Int. 134, 105271.

De Jager, A., Vogt, J., 2007. Rivers and catchments of Europe - catchment characterisation model (CCM). Eur. Comm. Jt. Res. Centre (JRC).

Desiante, W.L., Minas, N.S., Fenner, K., 2021. Micropollutant biotransformation and bioaccumulation in natural stream biofilms. Water Res. 193, 116846.

Di Marcantonio, C., Chiavola, A., Dossi, S., Cecchini, G., Leoni, S., Frugis, A., Spizzirri, M., Boni, M.R., 2020. Occurrence, seasonal variations and removal of organic micropollutants in 76 wastewater treatment plants. Process Saf. Environ. Prot. 141, 61–72.

Dummer, N.M., 2014. 4(5)-methylbenzotriazole: a review of the life-cycle of an emerging contaminant. Rev. Environ. Sci. Bio/Technol. 13 (1), 53–61.

Fenner, K., Canonica, S., Wackett, L.P., Elsner, M., 2013. Evaluating pesticide degradation in the environment: blind spots and emerging opportunities. Science 341 (6147), 752.

Fenner, K., Screpanti, C., Renold, P., Rouchdi, M., Vogler, B., Rich, S., 2020. Comparison of small molecule biotransformation half-lives between activated sludge and soil: opportunities for read-across? Environ. Sci. Technol. 54 (6), 3148–3158.

Fernández, M., Fernández, M., Laca, A., Laca, A., Díaz, M., 2014. Seasonal occurrence and removal of pharmaceutical products in municipal wastewaters. J. Environ. Chem. Eng. 2 (1), 495–502.

Fischer, H., Wanner, S.C., Pusch, M., 2002. Bacterial abundance and production in river sediments as related to the biochemical composition of particulate organic matter (POM). Biogeochemistry 61 (1), 37–55.

Gao, H., LaVergne, J.M., Carpenter, C.M., Desai, R., Zhang, X., Gray, K., Helbling, D.E., Wells, G.F., 2019. Exploring co-occurrence patterns between organic micropollutants and bacterial community structure in a mixed-use watershed. Environ. Sci. Process. Impacts 21 (5), 867–880.

Gonçalves, N.P.F., Iezzi, L., Belay, M.H., Dulio, V., Alygizakis, N., Dal Bello, F., Medana, C., Calza, P, 2021. Elucidation of the photoinduced transformations of Aliskiren in river water using liquid chromatography high-resolution mass spectrometry. Sci. Total Environ. 800, 149547.

Hamdhani, H., Eppehimer, D.E., Bogan, M.T., 2020. Release of treated effluent into streams: a global review of ecological impacts with a consideration of its potential use for environmental flows. Freshw. Biol. 65 (9), 1657–1670.

Hass, M., Davisson, J.W., 1977. Absorption coefficient of pure water at 488 and 541.5nm by adiabatic laser calorimetry*. J. Opt. Soc. Am. 67 (5), 622–624.

Helbling, D.E., Johnson, D.R., Honti, M., Fenner, K., 2012. Micropollutant biotransformation kinetics associate with WWTP process parameters and microbial community characteristics. Environ. Sci. Technol. 46 (19), 10579–10588.

Honti, M., Bischoff, F., Moser, A., Stamm, C., Baranya, S., Fenner, K., 2018a. Relating degradation of pharmaceutical active ingredients in a stream network to degradation in water-sediment simulation tests. Water Resour. Res. 54 (11), 9207–9223.

Honti, M., Bischoff, F., Moser, A., Stamm, C., Baranya, S., Fenner, K., 2018b. Relating degradation of pharmaceutical active ingredients in a stream network to degradation in water-sediment simulation tests. Water Resour. Res. 54 (11), 9207–9223.

Honti, M., Fenner, K., 2015. Deriving persistence indicators from regulatory water-sediment studies - opportunities and limitations in OECD 308 data. Environ. Sci. Technol. 49 (10), 5879–5886.

Honti, M., Hahn, S., Hennecke, D., Junker, T., Shrestha, P., Fenner, K., 2016. Bridging across OECD 308 and 309 data in search of a robust biotransformation indicator. Environ. Sci. Technol. 50 (13), 6865–6872.

IKSR (2019) Sondermessprogramm Chemie 2017, Bericht Nr. 257.

Jaeger, A., Posselt, M., Betterle, A., Schaper, J., Mechelke, J., Coll, C., Lewandowski, J., 2019. Spatial and temporal variability in attenuation of polar organic micropollutants in an urban lowland stream. Environ. Sci. Technol. 53 (5), 2383–2395.

Jaeger, A., Posselt, M., Schaper, J.L., Betterle, A., Rutere, C., Coll, C., Mechelke, J., Raza, M., Meinikmann, K., Portmann, A., Blaen, P.J., Horn, M.A., Krause, S., Lewandowski, J., 2021. Transformation of organic micropollutants along hyporheic flow in bedforms of river-simulating flumes. Sci. Rep. 11 (1), 13034.

Kahl, S., Kleinsteuber, S., Nivala, J., van Afferden, M., Reemtsma, T., 2018. Emerging biodegradation of the previously persistent artificial sweetener acesulfame in biological wastewater treatment. Environ. Sci. Technol. 52 (5), 2717–2725.

Klement, A., Kodešová, R., Bauerová, M., Golovko, O., Kočárek, M., Fér, M., Koba, O., Nikodem, A., Grabic, R., 2018. Sorption of citalopram, irbesartan and fexofenadine in soils: estimation of sorption coefficients from soil properties. Chemosphere 195, 615–623.

Kromkamp, J.C., Peene, J., 2005. Changes in phytoplankton biomass and primary production between 1991 and 2001 in the Westerschelde estuary (Belgium/The Netherlands). Hydrobiologia 540 (1), 117–126.

Kunkel, U., Radke, M., 2012. Fate of pharmaceuticals in rivers: deriving a benchmark dataset at favorable attenuation conditions. Water Res. 46 (17), 5551–5565.

Laszakovits, J.R., Berg, S.M., Anderson, B.G., O'Brien, J.E., Wammer, K.H., Sharpless, C. M., 2017. p-Nitroanisole/pyridine and p-nitroacetophenone/pyridine actinometers revisited: quantum yield in comparison to ferrioxalate. Environ. Sci. Technol. Lett. 4 (1), 11–14.

Le Guet, T., Hsini, I., Labanowski, J., Mondamert, L, 2018. Sorption of selected pharmaceuticals by a river sediment: role and mechanisms of sediment or Aldrich humic substances. Environ. Sci. Pollut. Res. 25 (15), 14532–14543.

Li, J., Zhang, H., 2017. Factors influencing adsorption and desorption of trimethoprim on marine sediments: mechanisms and kinetics. Environ. Sci. Pollut. Res. 24 (27), 21929–21937.

Li, Z., Sobek, A., Radke, M., 2016. Fate of pharmaceuticals and their transformation products in four small European rivers receiving treated wastewater. Environ. Sci. Technol. 50 (11), 5614–5621.

Meynet, P., Davenport, R.J., Fenner, K., 2020. Understanding the dependence of micropollutant biotransformation rates on short-term temperature shifts. Environ. Sci. Technol. 54 (19), 12214–12225.

Montforts, M.H.M.M., 2006. Validation of the exposure assessment for veterinary medicinal products. Sci. Total Environ. 358 (1), 121–136.

OECD (2000) Test No. 106: adsorption – desorption using a batch equilibrium method.

Peuravuori, J., 2012. Aquatic photochemistry of diclofenac in the presence of natural dissolved organic chromophoric material and nitrate. Int. J. Environ. Anal. Chem. 92 (13), 1470–1492.

Radke, M., Maier, M.P., 2014a. Lessons learned from water/sediment-testing of pharmaceuticals. Water Res. 55, 63–73.

Radke, M., Maier, M.P., 2014b. Lessons learned from water/sediment-testing of pharmaceuticals. Water Res. 55, 63–73.

Radke, M., Ulrich, H., Wurm, C., Kunkel, U., 2010. Dynamics and attenuation of acidic pharmaceuticals along a river stretch. Environ. Sci. Technol. 44 (8), 2968–2974.

Revitt, D.M., Balogh, T., Jones, H., 2015. Sorption behaviours and transport potentials for selected pharmaceuticals and triclosan in two sterilised soils. J. Soils Sediments 15 (3), 594–606.

Rodríguez-Murillo, J.C., Zobrist, J., Filella, M., 2015. Temporal trends in organic carbon content in the main Swiss rivers, 1974–2010. Sci. Total Environ. 502, 206–217.

Ruff, M., Mueller, M.S., Loos, M., Singer, H.P., 2015. Quantitative target and systematic non-target analysis of polar organic micro-pollutants along the river Rhine using high-resolution mass-spectrometry – Identification of unknown sources and compounds. Water Res. 87, 145–154.

Schwarzenbach, R.P., Escher, B.I., Fenner, K., Hofstetter, T.B., Johnson, C.A., Von Gunten, U., Wehrli, B., 2006. The challenge of micropollutants in aquatic systems. Science 313 (5790), 1072–1077.

Seller, C., Özel Duygan, B.D., Honti, M., Fenner, K., 2021. Biotransformation of chemicals at the water–sediment interface – toward a robust simulation study setup. ACS Environm. Au 1 (1), 46–57.

Shrestha, P., Junker, T., Fenner, K., Hahn, S., Honti, M., Bakkour, R., Diaz, C., Hennecke, D, 2016. Simulation studies to explore biodegradation in water-sediment systems: from OECD 308 to OECD 309. Environ. Sci. Technol. 50 (13), 6856–6864.

Southwell, R.V., Hilton, S.L., Pearson, J.M., Hand, L.H., Bending, G.D., 2020. Inclusion of seasonal variation in river system microbial communities and phototroph activity increases environmental relevance of laboratory chemical persistence tests. Sci. Total Environ. 733, 139070.

Storck, F.R., Skark, C., Remmler, F., Brauch, H.J., 2016. Environmental fate and behavior of acesulfame in laboratory experiments. Water Sci. Technol. 74 (12), 2832–2842.

Tixier, C., Singer, H.P., Oellers, S., Müller, S.R., 2003. Occurrence and fate of carbamazepine, clofibric acid, diclofenac, ibuprofen, ketoprofen, and naproxen in surface waters. Environ. Sci. Technol. 37 (6), 1061–1068.

Varga, L., Fenner, K., Singer, H., Honti, M., 2023. From market to environment – consumption-normalized pharmaceutical emissions in the Rhine catchment. ChemRxiv. https://doi.org/10.26434/chemrxiv-2023-f4rg6.

Winter, C., Hein, T., Kavka, G., Mach, R.L., Farnleitner, A.H., 2007. Longitudinal changes in the bacterial community composition of the danube river: a whole-river approach. Appl. Environ. Microbiol. 73 (2), 421–431.